Biomedical Signal Processing and Control 112 (2026) 108453

Contents lists available at ScienceDirect

Biomedical Signal Processing and Control

journal homepage: www.elsevier.com/locate/bspc

A markerless platform for automatic assessment of gait based on Human Pose Estimation: A proof of concept

Michele Boldo [a,1], Roberto Di Marco [a,*,1], Stefano Aldegheri [a], Enrico Martini [a], Michela Cosma [b], Alessio Baricich [c], Giulio Gasperini [d], Alessandro Picelli [e], Nicola Smania [e], Nicola Bombieri [a]

[a] Department of Engineering for Innovation Medicine, University of Verona, Strada Le Grazie, 15, 37134, Verona, Italy
[b] Azienda Ospedaliero-Universitaria di Ferrara, Physical Medicine Unit, Movement Analysis Laboratory, via Aldo Moro, 8, 44124, Cona, Italy
[c] Department of Health Sciences, University of Piemonte Orientale "Amedeo Avogadro", via Solaroli, 17, 28100, Novara, Italy
[d] Villa Beretta Rehabilitation Center, via N. Sauro, 17, 23845, Costa Masnaga, Italy
[e] Department of Neurosciences, Biomedicine and Movement Sciences, University of Verona, Piazzale Ludovico Antonio Scuro, 10, 37134, Verona, Italy

ARTICLE INFO

Keywords:
Human Pose Estimation
Observational Gait Analysis
Portable measurement device
Motion analysis

ABSTRACT

Instrumental and observational gait analysis are time-consuming and call for adequate operator training. The instrumental analysis calls for dedicated spaces, whilst observational analysis remains strongly operator dependant and subtle information may be missed, despite standardized tools can be adopted by clinicians (i.e., tables with specific features to be looked for in people walking). Markerless motion capture systems, such as pose estimation software based on convolutional neural networks and machine learning algorithms, may overcome the limitations of both the described approaches. This article presents a Markerless Automatic video-based platform for Gait Analysis (MaGA) that, given a predefined clinical tool and starting from the video recording of a person walking, computes the joint kinematics, identifies gait cycle sub-phases, perform a feature extraction and disentangles pathological from physiological walking via support vector machine algorithms, with linear and non-linear kernels.

Results reported linear and non-linear models performances in classifying and predicting severity of gait alterations at hip and knee joints, according to the Ranchos Los Amigos scale. The Mean Absolute Error ranged between 0.04 and 0.70 for linear models and was generally lower than 0.50 for non-linear models. F1-scores are generally above 0.70, with a few exceptions. The analysis of three example cases demonstrate the effectiveness of the method in evaluating sagittal hip and knee kinematics, highlighting agreements and a few discrepancies with expert evaluations taken as ground truth.

The proposed platform has the potential to be customized for the automatic assessment of individuals' gait based on various clinical evaluation tools, thereby addressing the common limitations associated with them. Future plans include conducting comprehensive technical and clinical trials to assess the platform's sensitivity under varying data collection conditions. Additionally, efforts will be made to establish a broader reference dataset, encompassing individuals with diverse disorders and varying levels of pathology severity.

1. Introduction

Instrumented Gait Analysis (iGA) is of paramount importance to objectively quantify motor impairments of people with neurological and orthopedic disorders, aiming to prevent loss of function [1] and level the relevant healthcare and rehabilitation costs [2]. Conventional iGA is performed with stereophotogrammetry and is complemented with force plates to assess both human motion kinematics and kinetics [3–6]. Its practice is highly time-consuming and calls for dedicated spaces and personnel. As an alternative, observational gait analysis (oGA) calls for video recording of people performing tasks and a clinical expert post-evaluating normal or abnormal patterns in specific phases of the motor task under analysis [7]. Beside the need for adequate operator training and a large amount of time to process the videos, oGA has been questioned for not being systematic, nor able to detect subtle motion deviations from normal gait [8]. Structured instruments and guidelines to evaluate videos have been developed to overcome

* Corresponding author.
E-mail address: roberto.dimarco@univr.it (R. Di Marco).
[1] These authors contributed equally to this work with their names given in alphabetic order.

https://doi.org/10.1016/j.bspc.2025.108453
Received 17 September 2024; Received in revised form 17 June 2025; Accepted 1 August 2025
Available online 14 August 2025

these latter limitations, but their validity is still questioned as they: (i) remain strongly operator dependant; (ii) might call for visual gait cycle phases segmentation, luckily inducing more evaluation bias; and (iii) are performed with low to moderate test-retest and inter-rater reliability [8,9].

Another valid option to monitor individuals' motor abilities is the use of markerless (ML) motion capture [10,11]. This approach requires a video recording of a motion task and a human pose estimation software, normally based on convolutional neural networks to track body *keypoints* [12]. For their peculiarities, ML systems can: (i) be used both within and beyond clinical settings with no need of specialized operators [11]; (ii) be considered as low-cost systems [13]; (iii) be free from stereophotogrammetry-related errors (such as soft-tissue artefact and marker misplacement due to landmarks misrecognition [14–16]); and (iv) save time on video-processing, producing timely-effective and yet reliable results [17,18].

Appropriateness of using ML techniques for clinical gait analysis has been tested [19–21]. Recently, ML systems were found to be an effective tool to assess human postural deformities [22,23], and human joint kinematics during overground walking, although ML-derived kinematics do not perfectly overlap canonical iGA kinematics [18].

For its potential, ML systems might be the rightful trade-off between iGA and oGA. Indeed, being able to systematically evaluate human joint kinematics, ML systems could be used to automatically fill the oGA scales, avoiding the operator influence and making them objective. Such an approach would potentially provide clinicians with a powerful tool to collect unbiased information on individuals motor abilities.

Toward this view, this paper presents a proof of concept for an automatic markerless low-cost video-based evaluation of a clinical tool for oGA. Clinical tools for oGA normally call for the segmentation of the gait cycle into the stance (St) and swing (Sw) phases, and 8 (or less) sub-phases [24]. Subsequently, a rater evaluates possible joint kinematics deviations from what are known to be the normal patterns in each sub-phase and provide a feedback based on standard sheets related to the specific tool. To achieve the research aim, we developed *MaGA* (Markerless automatic platform for Gait Analysis), a platform that computes the joint kinematics starting from video recording of walking, identifies gait cycle sub-phases, and automatically evaluates pathological from non-pathological patterns.

2. MaGA: Markerless automatic platform for Gait Analysis

A markerless automatic platform to be used for the objective evaluation of patients walking, would call for a number of functional blocks, independently from the considered clinical scale to be adopted: (i) the ML system, consisting of a camera and a Human Pose Estimation (HPE) software; (ii) the approach to estimate the Human Joint Kinematics; (iii) the algorithm to identify the gait cycle phases, within which clinicians normally check for coherence of the study case against the so-called "normal pattern"; and (iv) a block to decide whether the kinematic pattern can be considered normal or pathological. These blocks for MaGA are shown in Fig. 1 and presented in details in the following sections.

2.1. The ML system

MaGA collects motion data through a single-camera ML system, which consists of a RGB+Depth sensor and a HPE software. The sensor (an Intel RealSense D415 in the case of study) provides both conventional RGB images and depth information via active stereoscopic processing. The resolution is set to 848 × 480 pixels for both RGB and Depth cameras, with sampling rate equal to 60 fps and Field of View (FOV) 69° × 42°.

The HPE software detects and tracks the main human keypoints into the 3D space. Those include shoulder, hip, knee and ankle joint centers. We adopted the OpenPose [25] HPE with Body_25 convolutional neural network (CNN) (25 keypoints to represent the human body) trained with COCO [26] and MPII datasets [27].

2.2. Estimate of human joint kinematics

Differently from the routine practice when dealing with motion capture data, where points' trajectories are returned to the end user as time histories of 3D coordinates, the approach considered in this paper is the one proposed and verified in [18]. The detailed description to calculate the planar joint kinematics is given in [18], while a short description is provided below complemented by Fig. 2.

The trajectories of the keypoints, which are thought to approximate the joint centers, are mapped onto the camera image plane, resulting in 2D trajectories. Segments are then represented by lines connecting the keypoints of the joint of interest and its neighboring joints. Their relevant kinematics are finally calculated as the one-dimensional angle in the sagittal plane between two adjacent body segments [18]: a proximal segment ($prox$) and a distal segment ($dist$).

For instance, consider points A, B, and C representing the hip, knee, and ankle keypoints, respectively. The planar angle at point B — corresponding to the planar knee flexion/extension — is determined by constructing the unit vectors along the segments hip-knee ($\hat{ab}$) and knee-ankle ($\hat{bc}$).

In order to solve the sign ambiguity of the angle computed via the arccosine function, the proximal and distal segment coordinate systems were artificially built based on the segment link axes (e.g., the hip-knee $\hat{ab}$ link) and the normal to the image plane, computed as the normal to plane defined by $\hat{ab}$ and $\hat{bc}$. The obtained orientation matrices are then used to compute the relative rotation matrix between the proximal and distal segments to the joint, and decomposed using appropriate Euler/Cardan sequence [28].

Kinematics are then smoothed with a Savitzky-Golay filter (i.e., a moving window-based smoothing) and resampled to a fixed frequency equal to 60 Hz. This step is essential to address any potential fluctuations in camera sampling rates. Eventually, kinematics are filtered with a 4th-order zero-lag Butterworth low-pass filter with a cut-off equal to 6 Hz to remove high-frequency noise and outliers.

It is worth underlying that human joint kinematics calculated with the described approach and kinematics obtained from canonical 3D biomechanical models show differences associated both with technique-specific errors, and differences in bony segment pose definitions and angle calculation conventions (i.e., the use of 1D angles instead of Euler/Cardan angles) [18].

2.3. Automatic detection of the main gait events through video segmentation

MaGA implements the identification of gait cycle (GC) sub-phases as defined in [24,29], which is based on the identification of the foot-strike (FS) and foot-off (FO) events of gait (Fig. 3). FS and FO divide the gait cycle in stance (St, from FS to FO) and swing phase (Sw, from FO to subsequent FS of the same foot). The Algorithm 1 is used to identify FS and FO events from a video.

The algorithm evaluates the left (L) and right (R) side of a subject view separately. Since self-occlusions can sensibly reduce the joint information, the algorithm considers the walk cycle using the subject side which is faced to the camera.

To be robust to both pathological and physiological walking patterns, the algorithm uses the horizontal coordinate of the ankle (i.e., the x coordinate of the ankle joint center trajectory) as main feature. This is smoothed using a 2nd-order Savitzky-Golay lowpass filter, with a window size of 15 frames (line 1 of Algorithm 1). The x_{ankle} is then derived to obtain its velocity, which is filtered again with a 5th-order Butterworth filter (cutoff frequency set to 2 Hz). Similarly, the velocity is derived and filtered to obtain the horizontal component of the ankle acceleration (lines 2 and 3). Candidate instants for FS and FO events are identified looking for peak values of the acceleration signal (lines 4 and 5), in combination with acceleration and velocity signs. A reverse sign of acceleration with respect to the velocity indicates the ankle is stopping (FS event). Vice versa, when the signs of the two

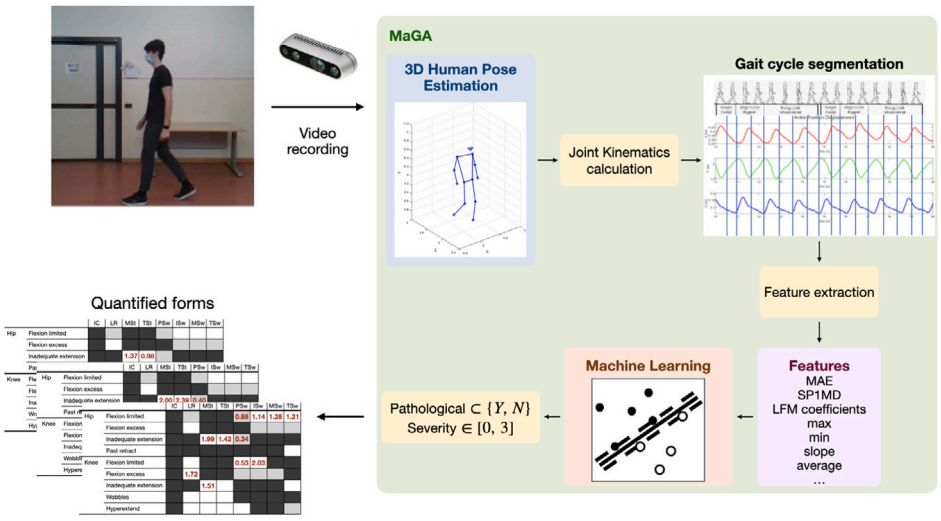

Fig. 1. Overview of platform pipeline.

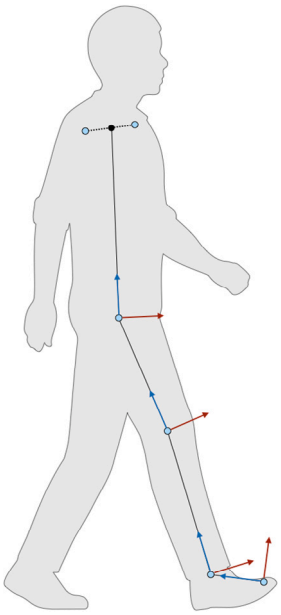

Fig. 2. Segments local coordinate systems built on the keypoints (light blue dots) and segment links (solid black lines).

signals match, the event is identified as FO (lines 7–27). The algorithm eventually check for the coherence of the sequence FS-FO-FS instants (lines 15–29): the first foot-strike, the successive foot-off, and the final foot-strike that begins a new gait cycle. To do so, the algorithm first sorts all the FS-FO candidates temporally (line 15). Then, a temporal-consistency check ensures the FS event is not override by a FO and vice versa.

If the combination of last remembered foot-strike (FS), last foot-off (FO) and current point (FS) is temporally coherent, then a 3-elements *cycle* (FS-FO-FS) is identified and returned (see Fig. 4).

It is important to note that the platform is modular, allowing the step segmentation algorithm to be replaced with alternatives depending on the specific use case. The unique requirement is that the alternative algorithms must extract the same features as those specified in Algorithm 1.

Algorithm 1 Automatic gait events detection

Require: $n \geq 0$
Require: $side \leftarrow L$ or R
1: $x \leftarrow lowpass(skeleton.ankle.x)$
2: $v, a \leftarrow get\_velocity(x), get\_acceleration(x)$
3: $p+, p- \leftarrow peaks(a), peaks(-a)$
4: $candidates \leftarrow []$
5: **for all** p in $p+$ **do**
6: **if** $(side = L \wedge v[p.idx] < 0) \vee (side = R \wedge v[p.idx] > 0)$ **then**
7: $append(candidates, [p.idx, FS])$
8: **end if**
9: **end for**
10: **for all** p in $p-$ **do**
11: **if** $(side = L \wedge v[p.idx] < 0) \vee (side = R \wedge v[p.idx] > 0)$ **then**
12: $append(candidates, [p.idx, FO])$
13: **end if**
14: **end for**
15: $candidates \leftarrow sort(candidates)$
16: $FS_{last}, FO_{last}, cycle \leftarrow -1, -1, []$
17: **for all** c in $candidates$ **do**
18: **if** c is FO **then**
19: $FO_{last} \leftarrow c$
20: **else if** c is FS **then**
21: **if** FS_{last} is too old w.r.t. c **then**
22: $FS_{last} \leftarrow c$
23: **end if**
24: **if** $FS_{last} < FO_{last} \wedge FO_{last} < c$ **then**
25: $append(cycle, [FS_{last}, FO_{last}, c])$
26: $FS_{last} \leftarrow c$
27: **end if**
28: **end if**
29: **end for**
30: **return** $cycle$

2.4. Gait cycle sub-phase identification

Given a foot-strike event at FS_i, a foot-off event at FO_i and the subsequent strike of the same foot at FS_{i+1}, gait cycle duration (t_{GC}), percentage of stance and swing phases duration over the gait cycle (P_{St}

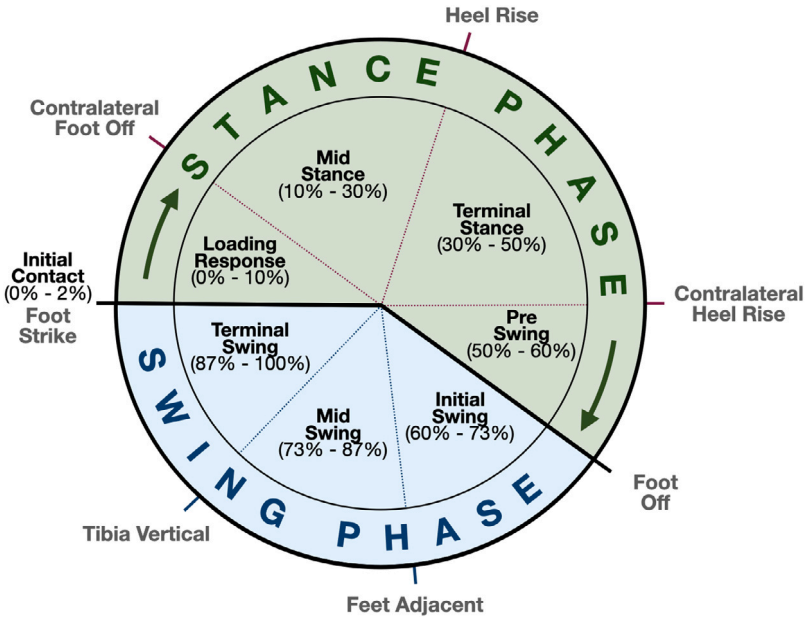

Fig. 3. Gait cycle phases with averaged physiological percentage.
Source: Adapted from [30].

and P_{Sw}, respectively) for the ith gait cycle are defined as follows:

$$\begin{aligned} t_{GC} &= FS_{i+1} - FS_i \\ P_{St} &= \frac{FO_i - FS_i}{t_{GC}} \\ P_{Sw} &= \frac{FS_{i+1} - FO_i}{t_{GC}} \end{aligned} \tag{1}$$

In normal walking, the duration of stance and swing phase given as the percentage of the gait cycle duration (P_{St} and P_{Sw}) correspond to 60% and 40%, respectively. Pathological conditions can significantly alter this proportion.

Stance and swing phases break down in 8 sub-phases [24], as also depicted in Fig. 3: stance phase – Initial Contact (IC), Loading Response (LR), Mid-Stance (MSt), Terminal Stance (TSt), and Preswing (PSw); and swing phase – Initial Swing (ISw), Mid-Swing (MSw), and Terminal Swing (TSw). These 8 sub-phases are identified by re-scaling their nominal duration with respect to stance and swing phases to their subject-specific duration, having considered the FS and FO events to define them. Algorithm 2 takes as input the three events of the ith gait cycle (i.e., the initial FS, the closing FS and the intermediate FO), and the duration of the original phases given as the percentage of the nominal gait cycle. Each single phase is re-scaled within the macro-phase it lies in: i.e., IC, LR, MSt, TSt and PSw for the stance phase; and the ISw, MSw and TSw for the swing phase. The resulting array contains the new percentage for that ith gait cycle.

Algorithm 2 Phase re-scaling

Require: $FS_i, FO, FS_{i+1}, phases$
$phases_{new} \leftarrow []$
$p_{ns} \leftarrow \frac{FO - FS_i}{FS_{i+1} FS_i}$
$p_s \leftarrow 0.6$
for all p in $phases$ **do**
  $p_{new}.type \leftarrow p.type$
  if $p.type$ in $[IC, LR, MSt, TSt, PSw]$ **then**
    $p_{new}.t_{start} \leftarrow \frac{p.t_{start}}{p_s} \times p_{ns}$
    $p_{new}.t_{end} \leftarrow \frac{p.t_{end}}{p_s} \times p_{ns}$
  else
    $p_{new}.t_{start} \leftarrow p_{ns} + \frac{p.t_{start} - p_s}{1 - p_s} \times p_{ns}$
    $p_{new}.t_{end} \leftarrow p_{ns} + \frac{p.t_{end} - p_s}{1 - p_s} \times p_{ns}$
  end if
  $append(phases_{new}, p_{new})$
end for
return $phases_{new}$

2.5. Feature extraction

In order to instruct and train a decision support block, *MaGA* calculates a few features comparing the test data with a dataset of physiological kinematic variables (i.e., a control dataset).

The control dataset consists of data gathered with the same equipment of the present study from eight healthy adults (6 males and 2 females, 28.0 ± 3.7 years old, body mass 68.1 ± 14.9 kg, height 1.73 ± 0.12 m) with no history of traumas or neuropathies, who walked on a 6 meter long pathway. The control dataset was previously presented in [18].

Kinematic time history from the test participant (addressed as test kinematics hereinafter), who the MaGA platform is fed with for its evaluation, is manipulated to get the portion within each gait cycle sub-phase, identified as previously described. Average, minimum, maximum, standard deviation values, range of motion (ROM) and average slope of the test kinematics are computed in each sub-phase. This set of features, providing the descriptive statistics of the test kinematics, are complemented with features describing the closeness and statistical difference from the reference control dataset.

Test kinematics are compared with the reference curve, obtained as the grand average from the control dataset, calculating the mean absolute error (MAE) and looking at the Linear Fit Method (LFM) coefficients [31]: the scaling factor ($scale$), the weighted averaged offset ($shift$), and the trueness (R^2) of the linear regression model between the test kinematics and the reference curve. A decrease in R^2 values shows the presence of time shift between the curves [32].

Test and reference kinematics were also statistically compared, using the 1D one-sample t-test ($\alpha = 0.05$) [33,34]. This test is based on the statistical parametric mapping (SPM), from the Random Field Theory [35], which is used to analyze statistical differences among continuous time histories (without reducing the test to summary metrics:

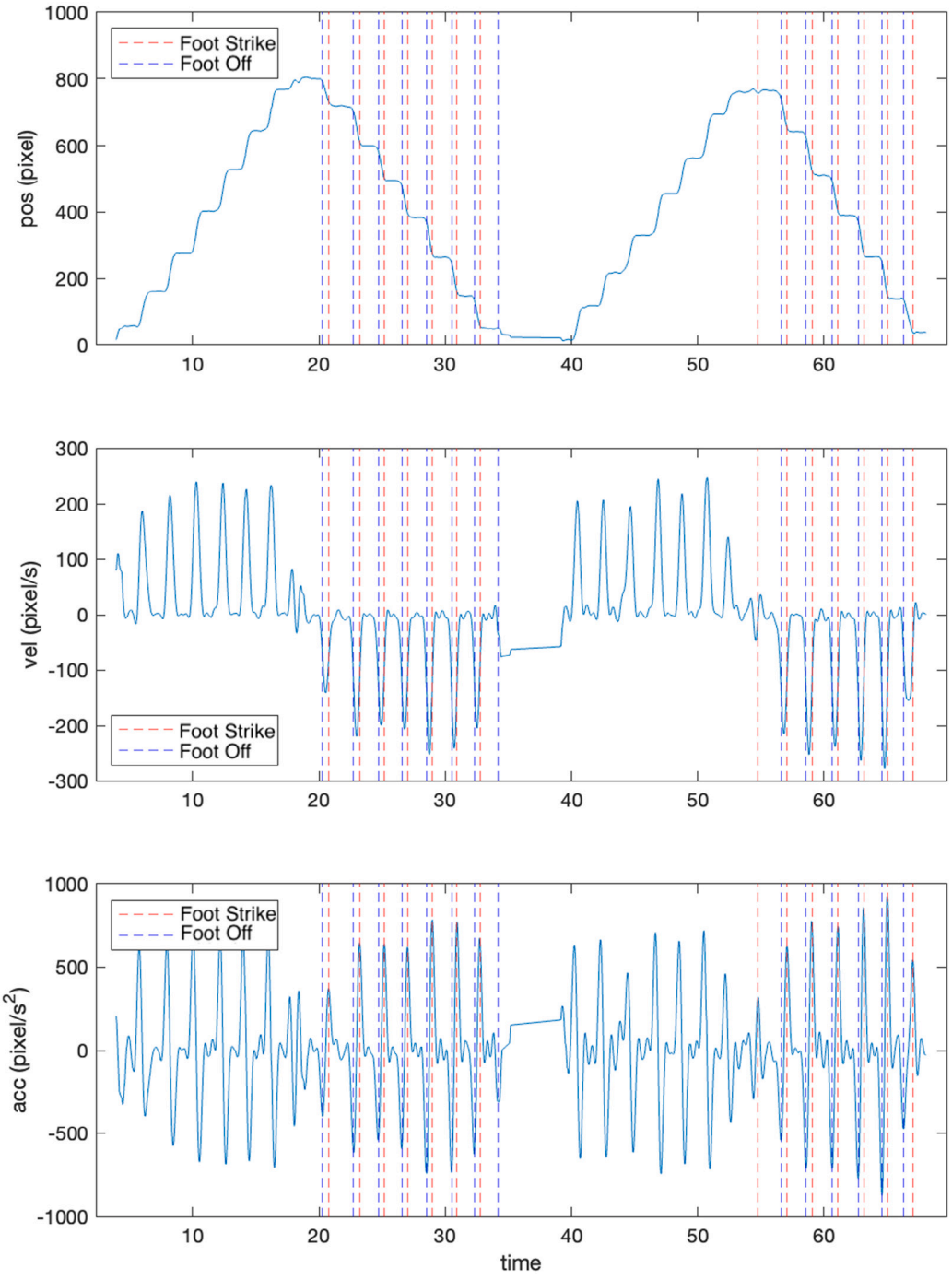

Fig. 4. Example of position (top plot), velocity (middle plot) and acceleration (bottom plot) of the x coordinate of the left ankle joint.

e.g., maximum or minimum values). This analysis was performed using the SPM1D open-source package for Python (spm1d.org) and returned, among others, the continuous t-value ($SPM\{t\}$), the t-limit (t^*), and the areas where differences were found ($p < 0.05$). The area under the $SPM\{t > t^*\}$ curve is calculated with numeric trapezoidal integration, and is used as additional feature to feed the decision support algorithm.

2.6. The decision support model

The extracted features are fed to a machine learning algorithm with the aim of predicting the likelihood of pathology severity within a specific gait sub-phase. To this purpose, we chose a *Support Vector Machine (SVM)*, trained for regression tasks.

A Support Vector Machine is a supervised machine learning algorithm widely used for classification and regression tasks. Its purpose is to determine an optimal hyperplane that separates classes or approximates a regression function by maximizing the margin between this hyperplane and neighboring points. SVMs can achieve excellent results for both linear and nonlinear separations and are also robust to outliers.

We tested Linear Support Vector Machines (implemented by Sklearn[2] Python library, regularization parameter $C = 1$), mainly to assess the significance of the extracted features, and RBF Gaussian

[2] https://scikit-learn.org/stable/

Kernel Support Vector Machines ($degree = 3$, $C = 1$) to optimize the accuracy of the results.

3. Materials and methods

3.1. Participants and ethic statement

Ten adults with a confirmed diagnosis of chronic stroke, recruited at the Rehabilitation Unit of the University Hospital of Verona "Borgo Roma" participated in this study (7 males and 3 females, 52.4 ± 9.5 years old, body mass 71.6 ± 11.2 kg, height 1.67 ± 0.09 m). Inclusion criteria comprehended: age greater than 18 years; hemiparesis consequent to first-ever unilateral ischemic or hemorrhagic stroke (subarachnoid hemorrhage excluded), documented by computerized tomography scan or magnetic resonance imaging; at least 6 months since stroke onset; ability to walk independently for at least 20 m, allowing the use of walking aids such as orthoses or cane. Participants were excluded if they participated in other trials or suffered from/had: severe cognitive impairment; other neurological or orthopedic conditions involving the lower limbs.

All participants read and signed an informed consent before participating in the study, which was performed in accordance with the Declaration of Helsinki and was approved by the Ethics Committee for Clinical Trials of Verona and Rovigo (Approval number 2320CESC, 04/Dec/2019).

Data gathered from participants of a previous study [18] was considered as control dataset to build the model and compare the patients' data with. Briefly, the control group consisted of eight healthy adults (6 males and 2 females, 28.0 ± 3.7 years old, body mass 68.1 ± 14.9 kg, height 1.73 ± 0.12 m).

3.2. Patients' evaluation

Participants were instructed to walk back and forth along a straight line overground, while being recorded by a lateral camera. They traveled a total of 10 walking tracks: 5 exposing the right side to the recording camera and 5 exposing the left side.

One of the most frequently cited clinical tool for oGA [36] is the Ranchos Los Amigos (RLA) [24], which calls for the segmentation of the gait cycle into the 8 sub-phases described in the previous sections [24]. A rater fills the standardized RLA sheet looking for joint kinematics deviations from the physiological patterns in each gait cycle sub-phase [24]. The RLA evaluates 38 kinematics features in a binary way (yes-no). Three of these are associated with trunk motion, 8 with the pelvis, 6 with the hip and 8 with the knee. Each feature aims to unravel functional impairments, possibly associated with tendon-muscle tension or laxity.

Toward the purpose of this study, and considering that RLA inter-rater reliability has been questioned [8,9], three expert physicians (MC, AB, GG) inspected the video-recording of walking of the participants with chronic stroke and filled the relevant RLA sheet. These sheets were used to train and test the MaGA platform adapted for RLA. Specifically, each cell of the cumulative RLA sheet was filled with:

- 0 if none of the experts raised concerns on the considered motion;
- 1 if one expert classified that observed motion as pathological;
- 2 if two experts classified that motion as pathological;
- 3 if all three agreed on classifying the observed motion as pathological.

Only gait alterations on the sagittal view were considered in this research. At least one participants exhibited one of the RLA items, enabling to build of a multi-class dataset for model training.

3.3. MaGA training, test and performance analysis

Data from healthy participants and those with pathologies were fed to the previously described MaGA platform and then used to train the machine learning models.

As mentioned, two types of SVM-based models were employed. The first has a linear kernel, allowing the actual use of features for the final prediction through relevance coefficients. The second model is a non-linear SVM with a Gaussian RBF kernel, allowing to leverage non-linearity and better approximate the regression function, possibly achieving more accurate results. Features have been scaled between the minimum and maximum values, so as to be ranging between 0 and 1.

Training and test were performed via a k-fold cross-validation approach, with $k = 10$. This methodology randomly shuffles and splits the dataset into k parts. The model is then trained on $k-1$ parts and tested on the remaining one, with the training-test process being iterated k times. The k-fold cross-validation was chosen as to cope with the high heterogeneity of the considered dataset (i.e., severity of the pathology was not the same across participants to allow having diverse RLA sheet fillings to train and test MaGA). Shuffling the data allows studying models' behavior across all cases.

The model returns both the normal/altered pattern of motion and the likelihood of the alteration on a continuous scale from 0 (i.e., the only value returning no altered pattern) to 3 (most likely altered pattern), The likelihood of detecting a movement alteration in a specific gait cycle sub-phase, hereinafter referred to as *likelihood*, is manually labeled considering the three expert evaluations: this is 0 if none of them would have reported alterations, while it is equal to 1, 2, or 3 if one, two, or all of them would have reported it.

The outcome of this system can be easily transformed into a classification task: likelihood tending approaching to 0 equals to the feature being labeled as normal, and labeled as altered otherwise. To each feature of the RLA sheet corresponds a model trained to recognize that specific feature and rate its likelihood.

Goodness of the performed classification as normal/altered walking of the testing subset was validated using the following metrics:

- **Accuracy *(Acc)*:** the ratio of correctly predicted instances to the total instances. It is a general measure of model correctness and is calculated as (TP + TN) / (TP + TN + FP + FN), where TP is True Positive, TN is True Negative, FP is False Positive, and FN is False Negative.
- **Precision *(Prec)*:** the ratio of correctly predicted positive observations to the total predicted positives. It measures the accuracy of the positive predictions and is calculated as TP / (TP + FP)
- **Sensitivity *(Sens)*:** is the ratio of correctly predicted positive observations to all observations in the actual class. It gauges the model's ability to identify all relevant instances and is calculated as TP / (TP + FN).
- **Specificity *(Specs)*:** the ability of the model to correctly identify negative instances. It is calculated as TN / (TN + FP).
- **F1 score (F1)**: the harmonic mean of precision and recall. F1 Score is calculated as:

$$F1 = 2 \cdot \frac{\text{Precision} \cdot \text{Sensitivity}}{\text{Precision} + \text{Sensitivity}} \tag{2}$$

The system ability to predict the likelihood of the identified gait alteration was evaluated using the **Mean Absolute Error *(MAE)***, representing the average of the absolute differences between the predicted and the actual values. Considering the 4 levels returned for alteration likelihood identification, the ideal upper limit for the MAE is 0.5, meaning that despite the prediction error, the system returns the right value. As an example, a patient who exhibit a gait alteration in a specific sub-phase of the gait cycle with likelihood 2 should be classified as pathological with a likelihood predicted value ranging between 1.5 and 2.5 by the system.

Table 1
Performances of the Support Vector Machine with the linear kernel built to evaluate the features of the hip joint kinematics.

Phase	Kinematic feature	Acc	Prec	Sens	Specs	F1	MAE
LR	Flexion Excess	0.91	0.89	0.60	0.98	0.70	0.27
MSt	Inadequate extension	0.91	0.86	0.96	0.88	0.91	0.52
TSt	Inadequate extension	0.95	0.95	0.94	0.96	0.94	0.60
PSw	Flexion Limited	0.78	0.82	0.22	0.99	0.33	0.34
PSw	Inadequate extension	0.71	0.81	0.44	0.92	0.52	0.35
ISw	Flexion Limited	0.89	0.90	0.79	0.94	0.84	0.54
ISw	Flexion Excess	0.96	0.82	0.87	0.97	0.82	0.24
MSw	Flexion Limited	0.88	0.84	0.83	0.90	0.83	0.60
MSw	Flexion Excess	0.94	0.84	0.70	0.98	0.72	0.22
TSw	Flexion Limited	0.77	0.81	0.59	0.90	0.65	0.52
TSw	Flexion Excess	0.90	0.73	0.29	0.99	0.41	0.13
TSw	Past Retract	0.85	0.08	0.04	0.99	0.05	0.16

Table 2
Performances of the Support Vector Machine with the non-linear kernel built to evaluate the features of the hip joint kinematics.

Phase	Kinematic feature	Acc	Prec	Sens	Specs	F1	MAE
LR	Flexion Excess	0.89	0.81	0.64	0.96	0.70	0.29
MSt	Inadequate extension	0.97	0.95	0.98	0.96	0.96	0.32
TSt	Inadequate extension	0.95	0.91	0.99	0.91	0.95	0.47
PSw	Flexion Limited	0.92	0.98	0.72	0.99	0.83	0.28
PSw	Inadequate extension	0.80	0.82	0.60	0.93	0.69	0.26
ISw	Flexion Limited	0.88	0.86	0.84	0.91	0.85	0.49
ISw	Flexion Excess	0.96	0.82	0.89	0.97	0.85	0.21
MSw	Flexion Limited	0.89	0.79	0.95	0.86	0.86	0.45
MSw	Flexion Excess	0.97	0.80	0.97	0.97	0.87	0.19
TSw	Flexion Limited	0.85	0.85	0.77	0.90	0.81	0.41
TSw	Flexion Excess	0.97	0.94	0.81	0.99	0.85	0.10
TSw	Past Retract	0.91	0.80	0.38	0.98	0.49	0.15

3.4. Case studies

To evaluate the performance of MaGA in a real-world scenario, we employed a leave-one-out approach. Specifically, the system was trained on 17 subjects (9 with pathological conditions and 8 healthy) out of a total of 18 in our dataset, and tested on the remaining excluded pathological subject. This procedure was repeated for all pathological subjects; however, for brevity, we report the results for three representative cases in the results section. This experimental design enables a qualitative analysis that is comparable to standard observational gait assessment.

4. Results

The Tables 1–4 show the performances of both linear and non-linear machine learning methods in classifying gait alterations at hip and knee joints, and predicting their likelihood. Tables 1 and 2 pertain to the hip flexion-extension angle, while Tables 3 and 4 show results obtained for knee flexion-extension angle. The MAE for the linear model ranged between 0.04 (Flexion Limited during MSw for the knee) and 0.54 (Flexion Limited during ISw for the hip), with the exception for the hip Inadequate extension in TSt and Flexion Limited in MSw reaching a MAE equal to 0.60, and the knee Flexion Excess in LR reaching a MAE equal to 0.70.

Classification goodness measured by the F1-score is generally larger than 0.70, with some exception both for hip and knee kinematics.

The non-linear model generally achieved better performances according to all metrics, with a MAE always lower than 0.50. The only exception was the knee Flexion Limited in LR with a MAE equal to 0.53. Similarly, the F1 was generally larger than 0.49 for the hip, with the lower limit reached for the Past Retract in TSw; and larger than 0.52 for the knee, with the lower limit reached for the Hyperextended item in LR.

Figs. 5 and 6 show the coefficients of a Linear Support Vector Machine trained for the items of hip Inadequate Extension in *TSt* and knee Hyperextension in *PSw*, respectively. The coefficients represent how important a feature is in the regression calculation. The further they deviate from 0, the more they influence the result.

4.1. Case studies results

Fig. 7 reports three case examples of MaGA application to the RLA sheet for the evaluation of sagittal hip and knee kinematics. Likelihood as estimated by MaGA and as obtained merging the experts' evaluations are reported if different from zero in each cell of the RLA sheet. In one of the examples, the knee Wobbles was not detected as a pathological feature in LR and MSt as highlighted by one of the three experts. For the other items in all cases there was agreement between MaGA and experts, although likelihood was different.

Table 3
Performances of the Support Vector Machine with the linear kernel built to evaluate the features of the knee joint kinematics.

Phase	Kinematic feature	Acc	Prec	Sens	Specs	F1	MAE
LR	Flexion Limited	0.73	0.68	0.33	0.92	0.39	0.53
LR	Flexion Excess	0.83	0.88	0.56	0.96	0.68	0.71
LR	Wobbles	0.84	0.33	0.13	0.99	0.17	0.20
LR	Hyperextend	0.85	0.67	0.10	1.00	0.18	0.16
MSt	Inadequate extension	0.91	0.94	0.83	0.96	0.88	0.59
MSt	Wobbles	0.98	0.99	0.91	1.00	0.95	0.10
MSt	Hyperextend	0.81	0.88	0.42	0.98	0.55	0.37
TSt	Hyperextend	0.97	0.92	0.91	0.98	0.91	0.22
PSw	Flexion Limited	0.88	0.79	0.97	0.82	0.87	0.41
PSw	Flexion Excess	0.90	0.96	0.52	0.99	0.62	0.21
PSw	Hyperextend	0.93	1.00	0.59	1.00	0.74	0.31
ISw	Flexion Limited	0.87	0.78	0.93	0.83	0.85	0.44
MSw	Flexion Limited	0.97	0.40	0.16	1.00	0.22	0.04
TSw	Inadequate extension	0.88	0.84	0.85	0.90	0.84	0.31

Table 4
Performances of the Support Vector Machine with the non-linear kernel built to evaluate the features of the knee joint kinematics.

Phase	Kinematic feature	Acc	Prec	Sens	Specs	F1	MAE
LR	Flexion Limited	0.79	0.72	0.62	0.87	0.65	0.53
LR	Flexion Excess	0.90	0.84	0.86	0.92	0.85	0.46
LR	Wobbles	0.90	0.83	0.55	0.98	0.65	0.15
LR	Hyperextend	0.88	0.81	0.41	0.98	0.52	0.17
MSt	Inadequate extension	0.95	0.94	0.95	0.96	0.94	0.36
MSt	Wobbles	0.96	0.92	0.87	0.98	0.89	0.09
MSt	Hyperextend	0.92	0.94	0.78	0.98	0.85	0.30
TSt	Hyperextend	0.99	0.96	0.96	0.99	0.96	0.12
PSw	Flexion Limited	0.92	0.86	0.93	0.90	0.90	0.28
PSw	Flexion Excess	0.93	0.86	0.80	0.96	0.82	0.16
PSw	Hyperextend	0.96	0.94	0.79	0.99	0.86	0.11
ISw	Flexion Limited	0.96	0.94	0.96	0.96	0.95	0.24
MSw	Flexion Limited	1.00	1.00	1.00	1.00	1.00	0.06
TSw	Inadequate extension	0.96	0.95	0.95	0.97	0.95	0.22

5. Discussions

Over the years, gait analysis has been widely recognized as a valuable tool for quantifying motor impairments in individuals with neurological and orthopaedic disorders, aiming to prevent loss of function and level the associated healthcare and rehabilitation costs [1, 2]. However, both instrumented (iGA) and observational gait analysis (oGA) present drawbacks that hamper their daily use in clinical facilities [7]. As an example, oGA tools have been questioned for their intrinsic low test-retest and inter-rater reliability [8,9], and the extensive training an operator would need before applying them.

The purpose of this research was to develop and present a proof of concept for a low-cost video-based platform (MaGA) to automatically use a clinical tool for observational GA, overcoming the proper limitations of human observations and training, and possibly paving the way to a more frequent use of objective and easy-to-use oGA in

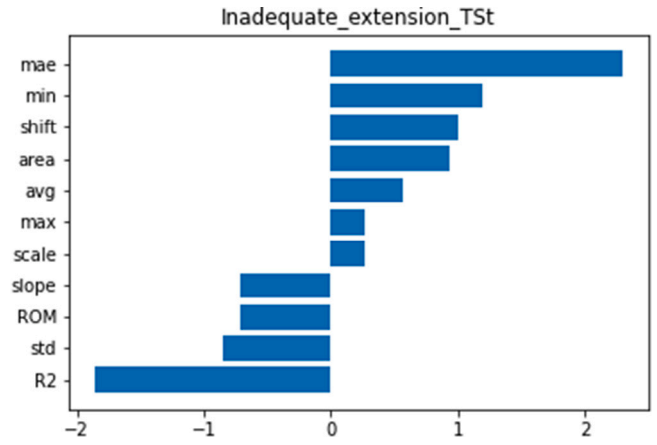

Fig. 5. Coefficients of the linear support vector machine used for regression of inadequate hip extension item during the terminal stance phase.

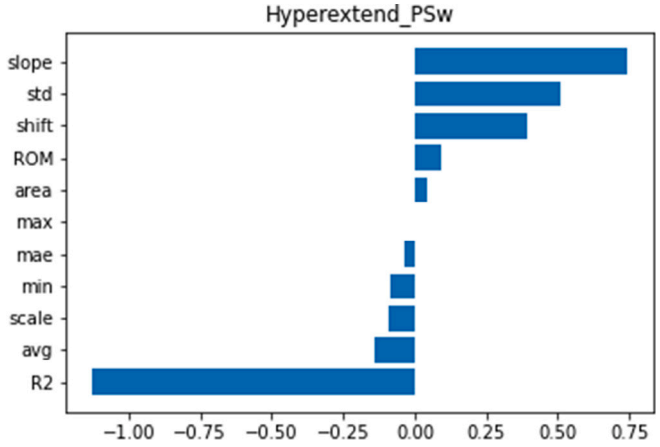

Fig. 6. Coefficients of the linear support vector machine used for regression of knee hyperextension item during the pre swing phase.

daily evaluation of people with motor disorders. To be considered automatic, an instrumental gait analysis system must require minimal human intervention. Therefore, we have developed a fully automated platform that covers the entire process from data acquisition to the compilation of the clinical scale. We have implemented a custom gait cycle segmentation algorithm, which, through experimental validation, we found to perform comparably to manual segmentation. The step segmentation algorithm is replaceable, and using a more accurate algorithm would possibly produce even more reliable results in the automatic compilation of the clinical scale. Despite being scalable to any clinical tool for oGA, the focus was paid to the application of MaGA to the Ranchos Los Amigos [24], which is among the mainly considered tools to assess and rate pathological gait of people [36].

Among the items of the RLA sheet, only sagittal kinematics of the hip and the knee were tested as paradigmatic examples to pursue the aims of the present study, as 3D kinematics and those pertaining to the ankle joints would not be reliably computed by the adopted Human Pose Estimator [18]. Each cell of the RLA sheet was associated with a trained machine-learning model based on a Support Vector Machine (SVM), implemented with both linear and non-linear kernels to evaluate and classify deviations in joint motion.

The choice of kernel significantly affected the model's performance. In general, the non-linear kernel yielded superior results across all evaluation metrics, including accuracy, precision, sensitivity, specificity, F1-score, and mean absolute error (MAE). Specifically, the non-linear models achieved MAE values consistently below 0.50 for nearly all gait deviations, with only one exception (knee Flexion Limited in LR, MAE = 0.53). In contrast, linear models occasionally exceeded this threshold, with values reaching up to 0.60 for hip Inadequate Extension in TSt and Flexion Limited in MSw, and up to 0.70 for knee Flexion Excess in loading response (LR). These findings suggest that non-linear SVMs are more effective in capturing the complex separable patterns in kinematic features associated with pathological gait.

Moreover, F1-scores obtained with the non-linear models were generally higher than those obtained with linear models, indicating better overall classification performance. While linear models showed F1-scores above 0.70 in most cases, exceptions were observed for certain gait abnormalities, especially those characterized by low prevalence or greater inter-subject variability. For instance, the linear SVM showed poor sensitivity and F1 in detecting hip Past Retract during TSw ($F1 = 0.05$) and knee Hyperextension in LR ($F1 = 0.18$), while the non-linear model improved these metrics to 0.49 and 0.52, respectively.

Importantly, low MAE values are crucial in the context of this study, where a continuous prediction of the gait abnormality is mapped onto discrete RLA categories, referred to as likelihood. A MAE larger than 0.50 implies that the predicted value may fall into an adjacent class, potentially resulting in a classification shift (e.g., from "normal" to "mildly altered") and leading to clinical misinterpretation. Indeed, having an SVM returning a likelihood equal to 2 for a specific kinematic feature and with a $MAE > 0.5$ would mean that the likelihood could be either ≤ 1.5 or ≥ 2.5, possibly leading to a switch between normal/altered feature classification when likelihood is equal to 1. The adoption of non-linear kernels helps mitigate this risk, making the system more robust and reliable for clinical decision-making.

These results support the use of non-linear SVMs as a preferable choice when developing interpretable models for automated gait assessment in clinical settings. The stability in performance and reduced error margins strengthen their potential to provide clinicians with accurate and quantitative feedback on specific kinematic impairments, fostering objective decision-making in the rehabilitation process.

The appropriateness of having considered the selected features to feed the SVM models with was tested by looking at Figs. 5 and 6. It is easy to observe that inadequate hip extension in *TSt* reflects a lower value for the hip extension angle than in normal gait, contributing to an increase in the average error (MAE) between the normal pattern and the tested curves. Furthermore, the considered curves will have different shapes, reflecting in different slopes, thereby affecting *min* and *shift*, with consequent reduction of the correlation index (R^2). Similarly, knee hyperextension during the *PSw* alters the extension angle value, changing the slope of the curve in that phase and, consequently, the R^2 index, which were found to be the most significant features for the SVM.

5.1. Case studies

The case studies reported in Fig. 7 show how the MaGA works for the RLA sheet. Comparing the merged evaluations performed by the experts on the three participants taken as paradigmatic examples, it is possible to highlight that MaGA was able to recognize all the items highlighted as pathological and to not obtain false positives. In one case, though, MaGA failed to detect the knee wobbles in LR and MSt as highlighted by one of the three experts. Being the knee wobble an irregular shuffling of the joint and not a proper kinematics deviation, this false negative could be avoided considering a more fit capturing of motion (i.e., considering capture devices that allow video recording at higher resolution and rate).

It is worth noticing that likelihood as estimated by MaGA does not match the likelihood calculated by merging the experts' evaluations, and it is generally underestimated. Despite being greater than 0 in accordance with the experts' evaluations, MaGA likelihood estimate needs to be further investigated.

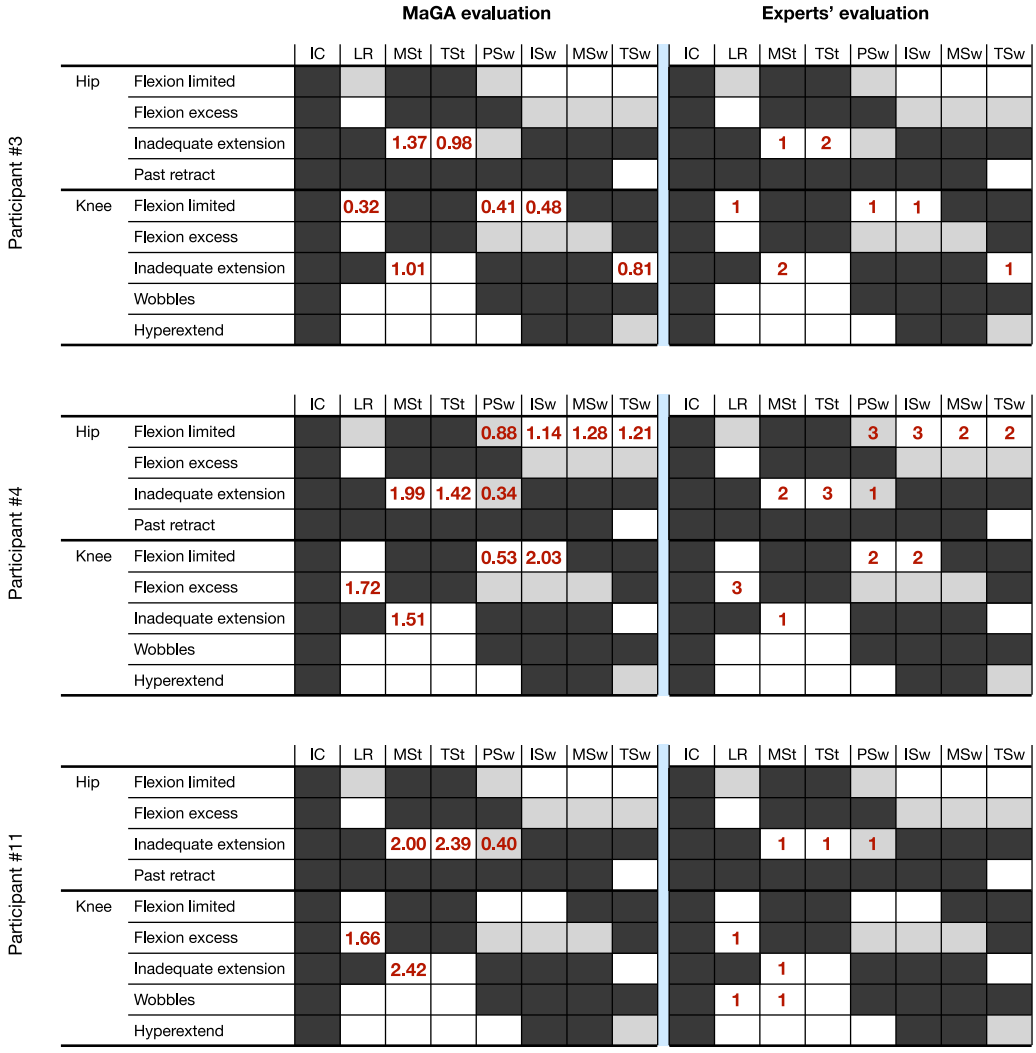

Fig. 7. MaGA-filled RLA sheet and experts' RLA evaluation obtained for three participants with chronic stroke for sagittal hip and knee joints. In black the non-relevant cells, in gray those with least relevance and in white the most relevant cells as provided in [24]. Likelihood, either calculated with MaGA (left hand side), or estimated summing the experts' evaluations (right hand side) is reported if different from zero in each cell.

5.2. Study limitations and future perspective

Although the aim of this research was to present a proof of concept for an automatic markerless low-cost video-based compilation of a clinical tool for oGA, it is important to acknowledge some limitations of the study. First, the small size of the dataset limits the generalizability of the findings. Since the proposed platform has not yet been validated for clinical use, further testing on larger and more diverse datasets is essential before considering any real-world applicability. Moreover, the evaluation was restricted to sagittal plane kinematics of the hip and knee, resulting in a partial assessment of the RLA sheet, which also includes 3D kinematics and ankle joint behavior that could not be reliably estimated with the current pose estimation approach. Finally, while a custom gait cycle segmentation algorithm was implemented, this was not validated, but its performance was only experimentally verified and found to be comparable to manual segmentation. It is worth noticing that this component is modular and replaceable, and the use of more accurate or clinically validated segmentation methods may further improve the reliability of the automatic compilation process and should be explored in future developments.

Ultimately, future research should focus on conducting a clinical trial with the aim of addressing the above limitations. This could enhance the model training and testing of the MaGA platform on a broader set of subjects for compiling the RLA sheet. The study protocol of the clinical trial should encompass a sensitivity analysis of MaGA to various data collection conditions and camera settings. These steps would contribute to a more comprehensive understanding of the platform's capabilities and reliability in diverse clinical scenarios.

6. Conclusion

The MaGA platform can potentially be adapted to automatically evaluate people gait according to any observational clinical assessment tool, overcoming the typical limitations associated with those (i.e, test-retest and inter-rater reliability). Future perspectives encompass an extensive technical and clinical trial to test the platform's sensitivity to the data collection conditions and define a wider reference dataset, composed by people with different disorders and pathology severity.

CRediT authorship contribution statement

Michele Boldo: Writing – review & editing, Writing – original draft, Visualization, Software, Methodology, Formal analysis, Conceptualization. **Roberto Di Marco:** Writing – review & editing, Writing –

original draft, Visualization, Supervision, Methodology, Formal analysis, Conceptualization. **Stefano Aldegheri:** Writing – review & editing, Software, Methodology, Conceptualization. **Enrico Martini:** Writing – review & editing, Methodology. **Michela Cosma:** Writing – review & editing, Investigation. **Alessio Baricich:** Writing – review & editing, Investigation. **Giulio Gasperini:** Writing – review & editing, Investigation. **Alessandro Picelli:** Writing – review & editing, Investigation, Conceptualization. **Nicola Smania:** Writing – review & editing, Project administration, Conceptualization. **Nicola Bombieri:** Writing – review & editing, Writing – original draft, Supervision, Project administration, Methodology, Conceptualization.

Declaration of competing interest

None declared.

Data availability

The authors do not have permission to share data.

References

[1] M.G. Benedetti, E. Beghi, A. De Tanti, A. Cappozzo, N. Basaglia, A.G. Cutti, A. Cereatti, R. Stagni, F. Verdini, M. Manca, et al., SIAMOC position paper on gait analysis in clinical practice: General requirements, methods and appropriateness. Results of an Italian consensus conference, Gait Posture 58 (2017) 252–260.

[2] M. van der Vlegel, J.A. Haagsma, A.J. Geraerds, L. de Munter, M.A. de Jongh, S. Polinder, Health care costs of injury in the older population: a prospective multicentre cohort study in the Netherlands, BMC Geriatr. 20 (1) (2020).

[3] A. Cappozzo, U. Della Croce, A. Leardini, L. Chiari, Human movement analysis using stereophotogrammetry. Part 1: theoretical background, Gait Posture 21 (2) (2005) 186–196, [Online]. Available: http://www.ncbi.nlm.nih.gov/pubmed/15639398.

[4] L. Chiari, U. Della Croce, A. Leardini, A. Cappozzo, Human movement analysis using stereophotogrammetry. Part 2: instrumental errors, Gait Posture 21 (2) (2005) 197–211, [Online]. Available: http://www.ncbi.nlm.nih.gov/pubmed/15639399.

[5] A. Leardini, L. Chiari, U. Della Croce, A. Cappozzo, Human movement analysis using stereophotogrammetry. Part 3. Soft tissue artifact assessment and compensation, Gait Posture 21 (2) (2005) 212–225, [Online]. Available: http://www.ncbi.nlm.nih.gov/pubmed/15639400.

[6] U. Della Croce, A. Leardini, L. Chiari, A. Cappozzo, Human movement analysis using stereophotogrammetry Part 4: Assessment of anatomical landmark misplacement and its effects on joint kinematics, Gait Posture 21 (2) (2005) 226–237.

[7] C. Rathinam, A. Bateman, J. Peirson, J. Skinner, Observational gait assessment tools in paediatrics–a systematic review, Gait Posture 40 (2) (2014) 279–285.

[8] H.R. Groth, S.E. Novak, Examination of the Reliability and Validity of Rancho Los Amigos Observational Gait Analysis (Ph.D. thesis), Grand Valley State University, 1999.

[9] C. Ridao-Fernández, E. Pinero-Pinto, G. Chamorro-Moriana, et al., Observational gait assessment scales in patients with walking disorders: systematic review, BioMed Res. Int. 2019 (2019).

[10] W.W. Lam, K.N. Fong, The application of markerless motion capture (MMC) technology in rehabilitation programs: a systematic review and meta-analysis, in: Virtual Reality, Springer Science and Business Media Deutschland GmbH, 2022.

[11] B. Scott, M. Seyres, F. Philp, E.K. Chadwick, D. Blana, Healthcare applications of single camera markerless motion capture: a scoping review, PeerJ 10 (2022).

[12] Z. Cao, T. Simon, S.-E. Wei, Y. Sheikh, Realtime multi-person 2d pose estimation using part affinity fields, in: Proceedings of the IEEE Conference on Computer Vision and Pattern Recognition, 2017, pp. 7291–7299.

[13] M. Ota, H. Tateuchi, T. Hashiguchi, N. Ichihashi, Verification of validity of gait analysis systems during treadmill walking and running using human pose tracking algorithm, Gait Posture 85 (2021) 290–297.

[14] V. Camomilla, R. Dumas, A. Cappozzo, Human movement analysis: The soft tissue artefact issue, J. Biomech. 62 (2017) 1–4, Human Movement Analysis: The Soft Tissue Artefact Issue, [Online]. Available: https://www.sciencedirect.com/science/article/pii/S0021929017304578.

[15] E. Scalona, R. Di Marco, E. Castelli, K. Desloovere, M.V.D. Krogt, P. Cappa, S. Rossi, Inter-laboratory and inter-operator reproducibility in gait analysis measurements in pediatric subjects, Int. Biomech. 6 (1) (2019) 19–33, PMID: 34042002.

[16] M. Fonseca, M. Bergere, J. Candido, F. Leboeuf, R. Dumas, S. Armand, The conventional gait model's sensitivity to lower-limb marker placement, Sci. Rep. 12 (1) (2022) 1–8.

[17] E. Martini, M. Boldo, S. Aldegheri, N. Valè, M. Filippetti, N. Smania, M. Bertucco, A. Picelli, N. Bombieri, Enabling gait analysis in the telemedicine practice through portable and accurate 3D human pose estimation, Comput. Methods Programs Biomed. 225 (2022) 107016.

[18] M. Boldo, R. Di Marco, E. Martini, M. Nardon, M. Bertucco, N. Bombieri, On the reliability of single-camera markerless systems for overground gait monitoring, Comput. Biol. Med. (2024) 108101.

[19] A. Ong, I.S. Harris, J. Hamill, The efficacy of a video-based marker-less tracking system for gait analysis, Comput. Methods Biomech. Biomed. Eng. 20 (10) (2017) 1089–1095.

[20] R. Tanaka, H. Takimoto, T. Yamasaki, A. Higashi, Validity of time series kinematical data as measured by a markerless motion capture system on a flatland for gait assessment, J. Biomech. 71 (2018) 281–285.

[21] E. D'Antonio, J. Taborri, I. Mileti, S. Rossi, F. Patane, Validation of a 3D Markerless System for Gait Analysis Based on OpenPose and Two RGB Webcams, IEEE Sens. J. 21 (15) (2021) 17064–17075.

[22] C.A. Artusi, C. Geroin, G. Imbalzano, S. Camozzi, S. Aldegheri, L. Lopiano, M. Tinazzi, N. Bombieri, Assessment of axial postural abnormalities in parkinsonism: Automatic picture analysis software, Mov. Disord. Clin. Pr. (2023).

[23] S. Aldegheri, C.A. Artusi, S. Camozzi, R. Di Marco, C. Geroin, G. Imbalzano, L. Lopiano, M. Tinazzi, N. Bombieri, Camera-and viewpoint-agnostic evaluation of axial postural abnormalities in people with parkinson's disease through augmented human pose estimation, Sensors 23 (6) (2023) 3193.

[24] J. Perry, Observational Gait Analysis Handbook, The Pathokinesiology Service and the Physical Therapy Department of Rancho Los Amigos Medical Center. Downey, CA: Loas Amigos Research and Education Institute Inc, 2001.

[25] Z. Cao, G. Hidalgo Martinez, T. Simon, S. Wei, Y.A. Sheikh, OpenPose: Realtime multi-person 2D pose estimation using part affinity fields, IEEE Trans. Pattern Anal. Mach. Intell. (2019).

[26] T.-Y. Lin, M. Maire, S. Belongie, J. Hays, P. Perona, D. Ramanan, P. Dollár, C.L. Zitnick, Microsoft coco: Common objects in context – version 3, https://arxiv.org/abs/1405.0312, Updated: 2015-02-21.

[27] M. Andriluka, L. Pishchulin, P. Gehler, B. Schiele, 2D human pose estimation: New benchmark and state of the art analysis, in: Proceedings of the IEEE Computer Society Conference on Computer Vision and Pattern Recognition, 2014, pp. 3686–3693.

[28] G. Wu, S. Siegler, P. Allard, C. Kirtley, A. Leardini, D. Rosenbaum, M. Whittle, D. D D'Lima, L. Cristofolini, H. Witte, et al., ISB recommendation on definitions of joint coordinate system of various joints for the reporting of human joint motion—part I: ankle, hip, and spine, J. Biomech. 35 (4) (2002) 543–548.

[29] J. Perry, Gait Analysis: Normal and Pathological Function, SLACK Incorporated, 1992.

[30] A. Leal-Junior, A. Frizera-Neto, Chapter 3 - gait analysis: overview, trends, and challenges, in: A. Leal-Junior, A. Frizera-Neto (Eds.), Optical Fiber Sensors for the Next Generation of Rehabilitation Robotics, Academic Press, 2022, pp. 53–64.

[31] M. Iosa, A. Cereatti, A. Merlo, I. Campanini, S. Paolucci, A. Cappozzo, Assessment of waveform similarity in clinical gait data: the linear fit method, BioMed Res. Int. 2014 (2014).

[32] R. Di Marco, E. Scalona, A. Pacilli, P. Cappa, C. Mazzà, S. Rossi, How to choose and interpret similarity indices to quantify the variability in gait joint kinematics, Int. Biomech. 5 (1) (2018) 1–8.

[33] T.C. Pataky, One-dimensional statistical parametric mapping in python, Comput. Methods Biomech. Biomed. Eng. 15 (3) (2012) 295–301.

[34] T.C. Pataky, Rft1d: Smooth one-dimensional random field upcrossing probabilities in python, J. Stat. Softw. 71 (7) (2016) 1–22, [Online]. Available: https://www.jstatsoft.org/index.php/jss/article/view/v071i07.

[35] K. Friston, J. Ashburner, S. Kiebel, T. Nichols, W. Penny (Eds.), Statistical Parametric Mapping – the Analysis of Functional Brain Images, Academic Press, London, 2007, pp. 625–647, [Online]. Available: https://www.sciencedirect.com/science/article/pii/B9780123725608500504.

[36] B. Toro, C. Nester, P. Farren, A review of observational gait assessment in clinical practice, Physiother. Theory Pr. 19 (3) (2003) 137–149.